İSTANBUL UNIVERSITY CERRAHPAŞA

ORIGINAL ARTICLE
Electrica 2023; 23(2): 338-344

Parametric Optimization of Double-Sided Printed Circuit Board With Triple Modal Reservation Accounting Failures

Artem V. Medvedev, Talgat R. Gazizov

Tomsk State University of Control Systems and Radioelectronics, Tomsk, Russian Federation

Cite this article as: A. V. Medvedev and T. R. Gazizov, "Parametric optimization of double-sided printed circuit board with triple modal reservation accounting failures," *Electrica*, 23(2), 338-344, 2023.

ABSTRACT

Modal reservation (MR) allows both increasing the circuit reliability and implementing the effect of modal filtering. The paper presents the study of a printed circuit board (PCB) with MR with the reference conductor in the form of side polygons. The structure is analyzed by quasi-static simulation, and the minimization of the maximum ultra-wideband pulse amplitudes at the far end of the structure after failures is first estimated. Using the heuristic search, the parameters for the PCB structure before and after failures are obtained. It is shown that, before failures, the maximum amplitude (U_{max}) does not significantly change under the condition of matching and at fixed values of loads. However, after failures, the U_{max} changes. For this structure, with increasing delay differences between pulses, U_{max} after failure 3 increased. It is shown that with obtained values of the geometric parameters, amplitudes of decomposition pulses change differently before and after failures. A prototype of the PCB was designed based on this study.

***Index Terms*—**Electromagnetic compatibility, ultra-wideband pulse, reliability, printed circuit board, failure, switching order

I. INTRODUCTION

To create reliable radioelectronic devices (REDs), it is necessary to pay close attention to functional safety and electromagnetic compatibility [1]. Unfortunately, REDs are prone to malfunctions, errors in operation, and even damage when exposed to electromagnetic interference. For example, ultra-wideband (UWB) pulses are especially dangerous for REDs because of their high penetration due to the short duration of exposure, high power, and wide spectrum [2], [3]. To protect against electromagnetic interference, there are various devices implemented on printed circuit boards (PCBs) [4], [5]. Reservation is a cardinal technique for improving reliability. Cold reservation is used in systems where high downtime is not as critical, but a high level of reliability is required.

Modal reservation (MR) is an approach to the layout and routing of reserving electrical interconnections, in which a strong electromagnetic coupling is formed between the reserved and reserving circuits [6]. This approach enables protecting electrical circuits from UWB pulse by means of modal distortions [7]. There are single and multiple (double, triple) MR solutions. Studies of structures with multiple MR have shown that, because of the difference in coupling between conductors, the order of switching is important [8], for instance, in the event of a failure simulated by either a short circuit (SC) or an open circuit (OC) at one of the ends of the reserved circuit. After switching to the reserving circuit, the maximum voltage of the decomposition pulses at the output changes. In the example for a microstrip line of four conductors, where conductor 1 is reserved, and conductors 2, 3, and 4 are reserving; if conductor 1 (active) fails, one of the reserving conductors can replace it and become active. However, the geometrical parameters of the cross-section can be such that the choice of the first conductor 3, and not 2 or 4, will allow for a greater attenuation at the output of the device [9]. Therefore, correct and efficient switching between conductors is advisable.

In this paper, we study a structure with a triple MR with the reference conductor in the form of side polygons [10]. Previously, its parametric optimization before failures was carried out according to the amplitude and time criteria [11]. However, the study did not take into account the fact

Corresponding author:
Artem V. Medvedev

E-mail:
medart20@rambler.ru

Received: May 26, 2022

Accepted: November 17, 2022

Publication Date: March 30, 2023

DOI: 10.5152/electrica.2023.22078

that the amplitude characteristics may change after failures. The purpose of the paper is to study the possibility of minimizing the maximum amplitude of the pulses at the output of the structure with a triple MR after failures and designing a PCB prototype based on this study. The novelty of this study lies in the fact that, in contrast to [10] and [11], the structures with MR are, for the first time, optimized taking into account failures.

II. STATEMENT OF THE PROBLEM

The TALGAT software [12] was used for the simulation. First, we created the cross-section of a PCB with an MR shown Fig. 1. Its parameters are the following: w is the width of the signal conductors, w_1 is the width of the reference conductors, s is the distance between the signal conductors, t is the thickness of the signal conductors, h is the thickness of the dielectric, d is the distance from the signal conductor to the reference one, and ε_r is the relative permittivity of the substrate. The initial set of cross-sectional parameters is as follows: $s = 150$ μm; $w = 700$ μm; $w_1 = 2000$ μm; $t = 18$ μm; $h = 600$ μm; $d = 800$ μm, and $\varepsilon_r = 9.8$.

Then, we calculated the matrices of per-unit-length coefficients of C and L inductances. Losses at this stage of the study were not taken into account; therefore, matrices **R** (for losses in conductors) and **G** (for losses in dielectrics) were assumed to be zero.

The cross-section has a reserved (C1) and three reserving (C2, C3, and C4) conductors, made in such a way that there is a strong electromagnetic coupling between them. The reference conductor is made in the form of lateral polygons on the left and right, interconnected by vias along the entire length of the structure. This way, the distance between the centers of adjacent vias (along conductors) is 2 mm. This structure is symmetrical, so the wave impedance for each conductor will be the same.

Next, we constructed an equivalent circuit for simulating a line with a length $l = 0.3$ m, loads (R1–R8 equal to 50 Ω). The excitation is in the form of a UWB pulse with an Electromotive force (EMF) amplitude of 2 V and a total duration of 150 ps.

Finally, the output voltage waveform was calculated in the range of given parameters according to the diagram in Fig. 2. In this diagram, R1, R3, R5, and R7 are the near-end resistances for one of the four conductors which is the active one. That is, if C1 is an active conductor, then R1 is the given near-end resistance, and R3, R5, and R7 are functioning as the near-end loads. Resistances R2, R4, R6, and R8 are loads at the far end of the structure. For the variant before failures, these resistances are matching the structure. In case of successive

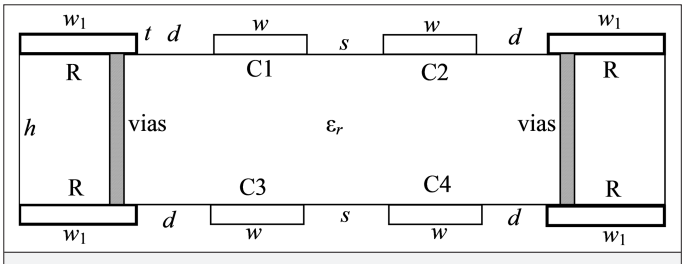

Fig. 1. Cross-section of a structure with MR, where C1–C4 are conductors and R is a resistance conductor. MR, modal reservation.

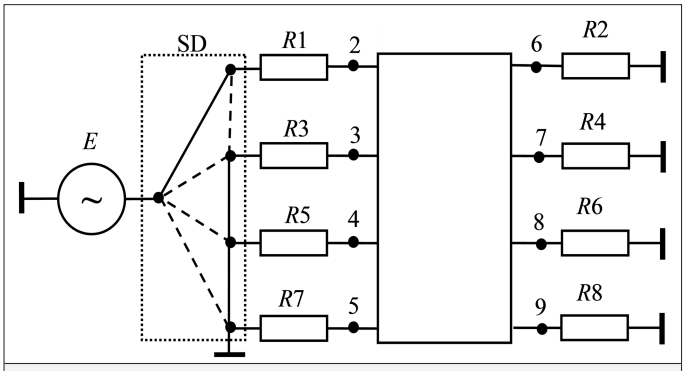

Fig. 2. Schematic of a structure with MR, where SD is a switching device.

failures (SC or OC) of each reserved circuit, it is assumed that the switching device transfers the functions of the reserved circuit to the reserving one. In simulation, the resistor values for the active conductor were chosen to be 50 Ω, and for the passive conductors, they were 50 Ω, 1 MΩ (OC), and 1 μΩ (SC) for various failure options [13].

Figure 3 shows a simplified diagram for choosing the active conductor after successive failures for symmetrical structures [14]. In such structures, it is possible to change the boundary conditions at the ends of the passive conductors rather than changing the active conductor. The total number of considered options for combinations of boundary conditions after failures was 62: 6, 24, and 32 options for cases after failures 1, 2, and 3, respectively.

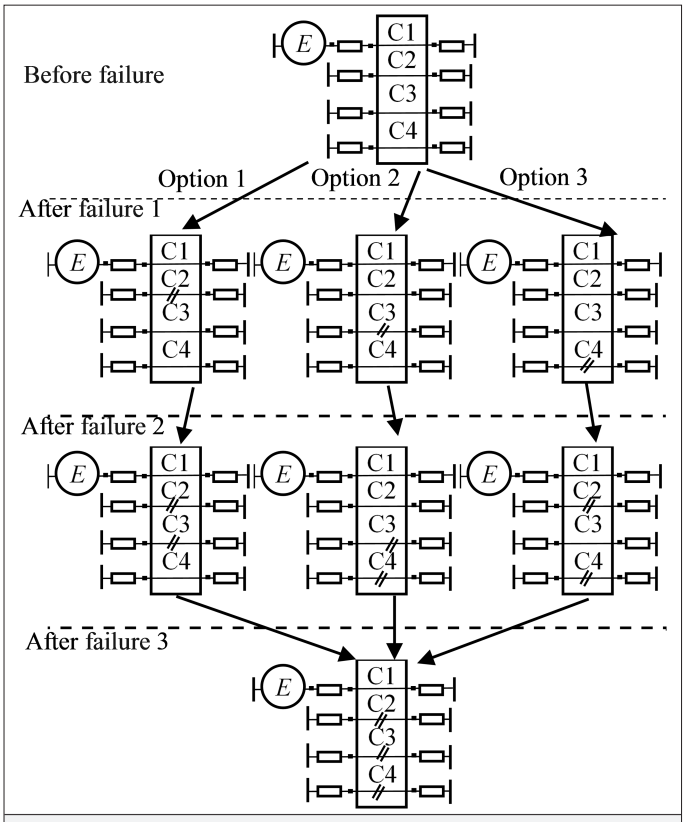

Fig. 3. Simplified diagram for choosing the active conductor.

III. SIMULATION RESULTS

Here, the optimization of the structure to failures was carried out by heuristic search, first by maximizing intervals and matching, and then by equalizing amplitudes and matching. Heuristic search optimization makes it possible to consider in detail the behavior of structure characteristics when changing parameters. In addition, because of the simplicity of the structure, it is not advisable to consider the structure with other optimization algorithms. Optimization according to the matching criterion allows the signal to be transmitted without distortion in the time domain. Optimization according to the maximum amplitude (U_{max}) minimization criterion makes it possible to increase the noise immunity of the structure. Optimization by the criterion of maximizing the intervals allows you to increase the duration of the noise pulse, which will be completely decomposed in this structure. However, achieving all three optimization criteria simultaneously is hard. Therefore, only some of them are used here. Matching was carried out for half the EMF for the voltage amplitude at the input of the structure. During optimization, the values of *w* varied in the range of 400–2000 μm, *s* in the range of 100–800 μm, *t* in the range of 18–130 μm, *h* in the range of 200–900 μm, and *d* in the range of 300–2000 μm. The optimized parameters of the cross-section are presented in Table I.

To analyze the time responses of the structure before and after failures, we used a UWB pulse excitation with a total duration of 0.15 ns and an EMF amplitude of 2 V. Then, the UWB pulse was excited to the near end of the reserved conductor (node 2 in Fig. 2). The voltage waveforms at the far end of the reserved conductor (node 6) were analyzed before and after failure. Figure 4 shows the pulse waveforms at the structure output before failures with the parameter sets before and after optimization from Table I. For the optimized parameter set 1, the delays are 1.51, 1.87, 2.28, and 2.7 ns, and for set 2, they are 1.85, 2.03, 2.25, and 2.51 ns for pulses 1, 2, 3, and 4, respectively. The minimum delay difference is 0.36 and 0.18 ns for sets 1 and 2, respectively. It can be seen that before failures, U_{max} is approximately the same for the original and two optimized sets of parameters and is equal to 0.25 V each.

TABLE I. SETS OF OPTIMIZED PARAMETERS FOR AMPLITUDE EQUALIZATION AND MATCHING (1) AND INTERVAL MAXIMIZATION AND MATCHING (2)

Parameter Set	*w*, μm	*s*, μm	*d*, μm	*h*, μm	*t*, μm
1	850	250	1800	600	130
2	800	600	500	1000	130

d, distance from the signal conductor to the reference one; *h*, thickness of the dielectric; *s*, distance between the signal conductors; *t*, thickness of the signal conductors; *w*, width of the signal conductors.

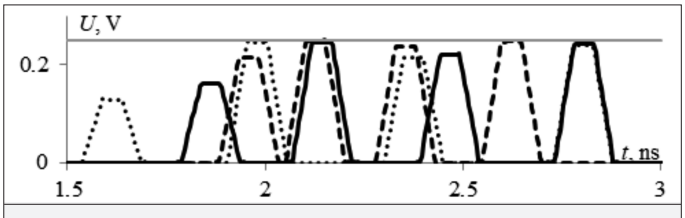

Fig. 4. Voltage waveforms at the far end of the structure with the initial (- -) and optimized parameter sets 1 (•••) and 2 (––) before failures.

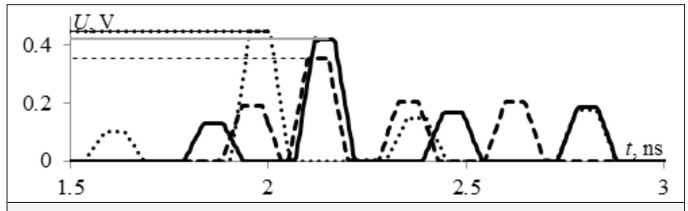

Fig. 5. Voltage waveforms at the far end of the structure with the initial (- -) and optimized parameter sets 1 (•••) and 2 (––) after failures.

Now, let us consider how the structure behaves after failures with the parameters obtained after optimization performed before failures. Figure 5 shows the pulse waveforms at the structure output after failures with parameter sets before and after optimization. After failures, the cases of 50-SC on C2, OC-50 on C3, and SC-50 on C4 (failure 3) are discussed, in which U_{max} is the largest of the 32 considered options. U_{max} for parameter sets before optimization, after optimization 1, and after optimization 2 are equal to 0.41, 0.448, and 0.355 V, respectively. This suggests that the amplitude after failures does not change uniformly.

A detailed description of the changes in responses after failures at one of the ends of the active conductor is presented in detail in [10] and omitted here. In what follows is their short clarification. After failures, the amplitude of each of the four decomposition pulses (Fig. 6) at the far end of the active conductor changes. In this case, U_{max} increases for each combination of OC, SC, and 50 Ω (Fig. 7). At the near end of the structure, a line mismatch will be observed, and in some cases, the amplitude will decrease or increase. As for the far end, the task is to find, after each failure, the switching option, in which the largest of the considered U_{max} will be the smallest of the three.

For all parameter sets, switching option 3 is optimal, since U_{max} is minimal for this option. Figures 6 and 7 show the relationship between U_{max} at the optimal switching order for the structure with the initial and optimized sets 1 and 2 and the failures at the far and near ends of the structure. It can be seen that after failure 3 for set 2, U_{max} is minimal and equal to 0.355 V. This is 8.3% and 12% less than for the initial set of parameters and optimized set 1, respectively. For Fig. 7, the upper line indicates the maximum increase, and the lower line, the maximum decrease in amplitude at the near end of the structure. The smallest range of amplitude change at the near end of the structure is observed for set 2 and is 0.086 V. This is 55% and 67% less than for the initial set of parameters and optimized set 1, respectively.

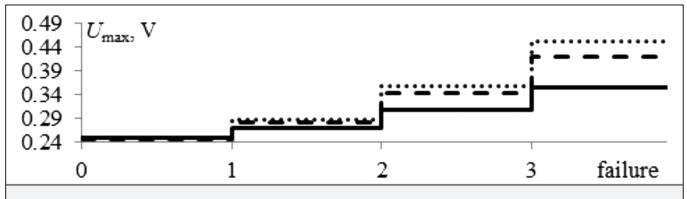

Fig. 6. Relationship between the type of failure and U_{max} at the far end of the structure with the optimal switching order for the structure with the initial (- -) and optimized sets 1 (••) and 2 (––). U_{max}, maximum amplitude.

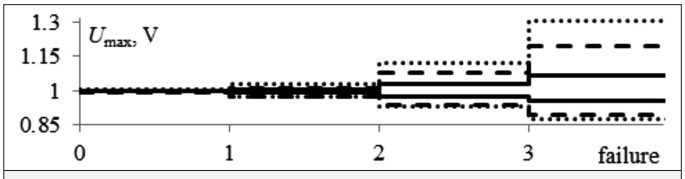

Fig. 7. Relationship between the type of failure and U_{max} at the near end of the structure with the optimal switching order for the structure with the initial (- -) and optimized sets 1 (••) and 2 (––).U_{max}, maximum amplitude.

Here, the structure was optimized after failures. In Table II, we present the relationship between the geometrical parameters and the voltages (U) of 1, 2, 3, and 4 pulses before and after failure 3, at which U_{max} is maximum (50-SC on C2, OC-50 on C3, and SC-50 on C4). After failures, the amplitudes of decomposition pulses change, since the energy in pulses is redistributed because of the reflections from loads. However, the difference between the minimum and maximum values in the parameter range varies for some modes. So, for example, for mode 2, when the parameter w changes before and after failures, this difference is 0 and 0.1 V, which is 0% and 12%, respectively. Such a difference is observed for almost all modes, but it is less significant. Thus, the pulse amplitudes do not change uniformly before and after failures. It is logical to optimize the structure after failures separately according to the amplitude criteria.

Optimization was carried out by heuristic search according to two criteria: U_{max} minimization and matching, in the same ranges as in the previous section. The optimized parameters were the following: $s=700$ μm; $w=900$ μm; $t=130$ μm; $h=600$ μm; $d=500$ μm, and $\varepsilon_r=9.8$. Figures 8 and 9 show the relationship between the optimized set after failure 3 and U_{max} at the optimal switching order for the structure with optimized set 2 before failures (with the best amplitude characteristics after failures). It can be seen that after failure 3 for the optimized set after failure 3, U_{max} is minimal and equal to 0.333 V. This is 3.2% less than for the optimized set 2.

The range of the amplitude changes at the near end of the structure for the optimized set after failure 3 is 0.066 V. This is 13% less than for the optimized set 2 before failures. Thus, optimization of the structure after failures in this case makes it possible to reduce U_{max} by

TABLE II. RELATIONSHIP BETWEEN PULSE AMPLITUDES (U) 1 (—), 2 (––), 3 (- -), AND 4 (••••) BEFORE AND AFTER FAILURE 3 (50-SC ON C2, OC-50 ON C3, SC-50 ON C4) AND VARIOUS GEOMETRICAL PARAMETERS

Before Failures	**After Failure 3**
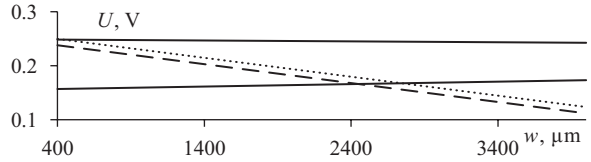	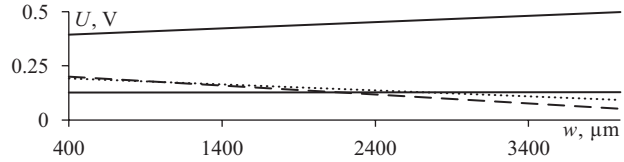
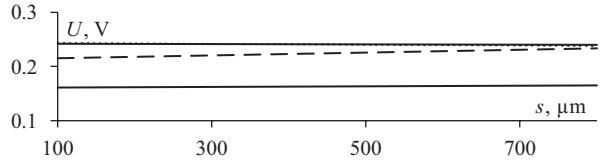	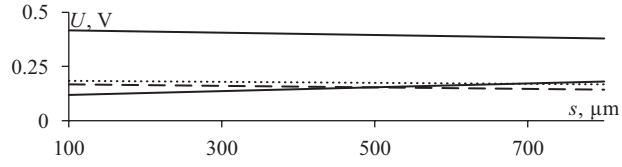
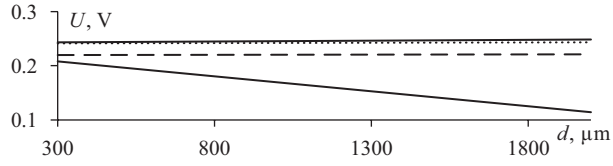	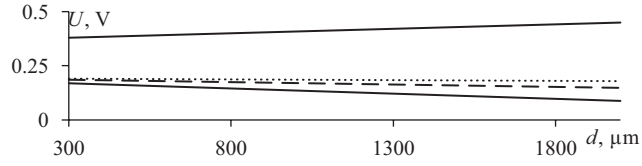
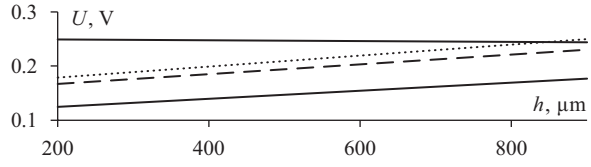	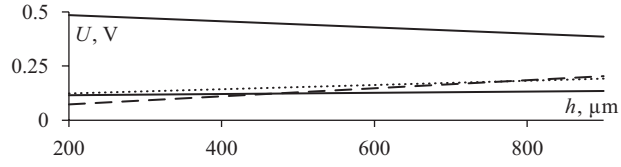
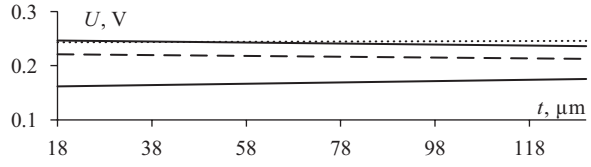	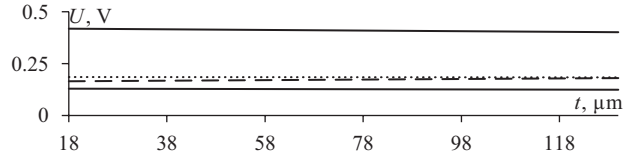

OC, open circuit; SC, short circuit.

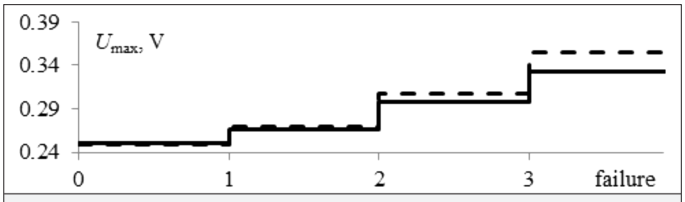

Fig. 8. Relationship between the type of failure and U_{max} at the optimal switching order for the structure with an optimized set 2 before failures (- -) and an optimized set after the failure (––) at the far end of the structure.

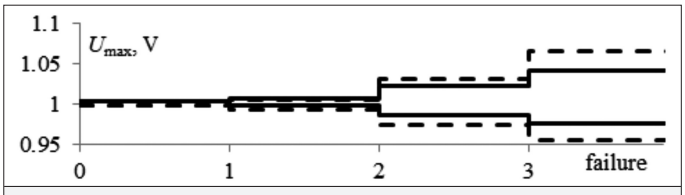

Fig. 9. Relationship between the type of failure and U_{max} at the optimal switching order for the structure with an optimized set 2 before failures (- -) and an optimized set after the failure (––) at the near end of the structure.

13% compared to optimization before failures. This will increase the probability of failure-free operation throughout the entire working life cycle of the MR system. Therefore, optimization of structures with MR after failures is more efficient than optimization before failures.

Finally, a prototype of a double-sided PCB with MR was developed. The topology of the PCB layers is shown in Fig. 10. To manufacture the layout, tracing was made using the positive method. The resulting PCB layers are shown in Fig. 11.

As the material of the dielectric substrate, we used aluminum oxide Al_2O_3 with a material purity of 98%. Such a material has the following technical characteristics: the thermal conductivity of 30 W/mK, the dielectric constant of 9.8 ± 0.1, the dielectric loss tangent of 0.0003, and the dielectric strength of 22 kV/mm. The prototype, excluding connectors, had dimensions of 320×200 mm. Other dimensions are given in Table III. Parameter sets 1 and 3 were optimized to maximize

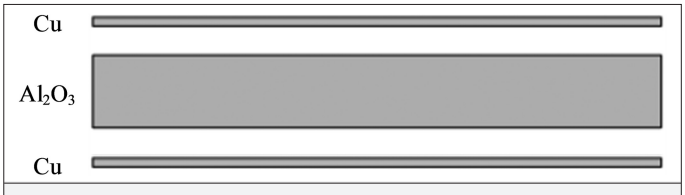

Fig. 10. Stack of a PCB prototype.

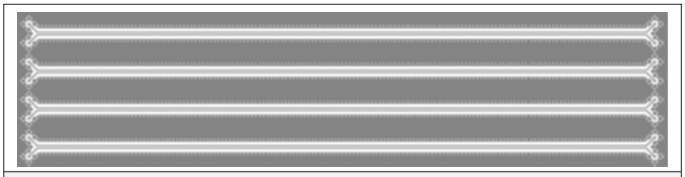

Fig. 11. Upper and lower layers of the PCB prototype.

TABLE III. GEOMETRICAL PARAMETERS OF THE PCB PROTOTYPE

Parameter Set	*w*, μm	*s*, μm	*d*, μm	*h*, μm	*t*, μm
1	850	250	1800	600	130
2	900	700	500		
3	950	150	1700		
4	1000	600	400		

d, distance from the signal conductor to the reference one; *h*, thickness of the dielectric; PCB, printed circuit board; *s*, distance between the signal conductors; *t*, thickness of the signal conductors; *w*, width of the signal conductors.

spacing and provide matching, while sets 2 and 4 were optimized to equalize amplitudes and provide matching.

To connect the measuring equipment and loads to the regular part of the PCB, we used Sub multi assembly (SMA) connectors of the 0732511350 brand. Since the PCB topology does not allow them to be connected directly (without violating the regularity of the PCB), we used embranchments with a length of no more than 5 mm.

IV. CONCLUSION

The results of the quasi-static simulation of the two-sided PCB with a triple MR have been presented. Using the heuristic search, the PCB parameters before failures and after failures were obtained. It is shown that, before failures, U_{max} does not significantly change under the matching condition and at fixed load values. However, after failures, the maximum amplitude changes. For this structure, with an increase in the intervals between pulses, U_{max} after failure 3 increased. It is demonstrated that when the values of the geometric parameters change, the pulse voltages change differently before and after failures. The PCB prototype has been developed based on this study.

Peer-review: Externally peer-reviewed.

Author Contributions: Concept – A.V.M.; Design – A.V.M.; Supervision – A.V.M.; Funding – T.R.G.; Materials – T.R.G.; Data Collection and/or Processing – A.V.M.; Analysis and/or Interpretation – A.V.M.; Literature Review – A.V.M.; Writing – A.V.M.; Critical Review – T.R.G.

Declaration of Interests: The authors have no conflicts of interest to declare.

Funding: The reported study was funded by Russian Science Foundation (project no. 20-19-00446) in TUSUR.

REFERENCES

1. M. R. Patel, *Spacecraft Power Systems*. Boca Raton, USA: CRC Press, 2005.
2. L. N. Zdoukhov, Yu. V. Parfenov, O. A. Tarasov, and V. M. Chepelev, "Three possible mechanisms for the failure of electronic devices as a result of electromagnetic interference [In Russian]," *Joint Inst. High Temp. Russ. Acad. Sci.*, vol. 2, pp. 22–34, 2018.
3. N. Mora, F. Vega, G. Lugrin, F. Rachidi, and M. Rubinstein, "Study and classification of potential IEMI sources," *System Design and Assessment Notes*, vol. 41, p. 1–92, 2014.
4. D. Borah, and T. S. Kalkur, "A planar multiband balanced bandstop filter," 2018 IEEE MTT-S Latin America Microwave Conference (LAMC 2018). pp. 1–3, 2018. [CrossRef]
5. D. Borah, and T. S. Kalkur, "Reconfigurable balanced dualband bandstop filter," vol. 2020, pp. 1–2, 2020. [CrossRef]

6. V. R. Sharafutdinov, and T. R. Gazizov, "Analysis of reservation methods based on modal filtration [In Russian]," *Syst. Control. Commun. Sec.*, vol. 3, pp. 117–144, 2019.
7. A. T. Gazizov, A. M. Zabolotsky, and T. R. Gazizov, "UWB pulse decomposition in simple printed structures," *IEEE Trans. Electromagn. Compat.*, vol. 58, no. 4, pp. 1136–1142, 2016. [CrossRef]
8. E. Genender, H. Garbe, and F. Sabath, "Probabilistic risk analysis technique of intentional electromagnetic interference at system level," *TEMC*, vol. 56, pp. 200–207, 2014.
9. F. Brauer, and J. Haseborg, "SPICE simulations and measurement techniques for protection circuits against UWB and HPM signals," *Book Admin. EUROEM*, vol. 3, pp. 1–23, 2008.
10. A. O. Belousov, A. V. Medvedev, E. B. Chernikova, T. R. Gazizov, and A. M. Zabolotsky, "Switching order after failures in symmetric protective electrical circuits with triple modal reservation," *Symmetry*, vol. 13, no. 6, pp. 1–22, 2021. [CrossRef]
11. P. E. Orlov, and E. Buichkin, "Method of assembling multi–layer printed circuit boards for circuits with reservation," *Proc. of the EDM*, vol. 2016, pp. 155–158, 2016.
12. S. P. Kuksenko, "Preliminary results of TUSUR University project for design of spacecraft power distribution network: EMC simulation," *IOP Conf. S. Mater. Sci. Eng.*, vol. 560, no. 1, pp. 1–7, 2019. [CrossRef]
13. A. V. Medvedev, "Studying the switching order for a three-wire structure with modal reservation after failure," IOP Conference Series: Materials Science and Engineering. vol. 919(2020), pp. 1–6, 2020.
14. P. E. Orlov, and V. R. Sharafutdinov, "Optimization of stack parameters of a multi-layer printed circuit board for circuits with redundancy by genetic algorithm," Pro. 2017 IEEE 2017 Int. Multi-Conf. on Eng., Comp. and Inform. Sciences. Novosibirsk, Russia. pp. 495–500, 2017.

Artem V. Medvedev was born in Tomsk, Russia, in 1994. He received the B.Sc. and M.Sc. degrees in Radio Engineering and Electromagnetic Compatibility from the Tomsk State University of Control Systems and Radioelectronics, Tomsk, Russia, in 2017 and 2019, respectively. Currently, he is a PhD student in electromagnetic compatibility of radioelectronic devices. He has over 4 years of experience with electromagnetic compatibility issues. His current research interests include electromagnetic compatibility, redundancy, and functional safety. He has authored or coauthored over 26 refereed publications.

Talgat R. Gazizov was born in Jalal-Abad, Kyrgyzstan, in 1963. He received the PhD degree in improvement of circuit board interconnections and the D.Sc. degree in reduction of electric signal distortion in the interconnections and effects of power electromagnetic interference from Tomsk State University of Control Systems and Radioelectronics, Tomsk, Russia, in 1999 and 2010, respectively. He has authored/coauthored more than 360 scientific papers, including 11 books. His research interest includes signal integrity problem.